UNIVERSITY OF COPENHAGEN

Exercise-Mediated Lowering of Glutamine Availability Suppresses Tumor Growth and Attenuates Muscle Wasting

Pedersen, Katrine S.; Gatto, Francesco; Zerahn, Bo; Nielsen, Jens; Pedersen, Bente K.; Hojman, Pernille; Gehl, Julie

iScience

Article

Exercise-Mediated Lowering of Glutamine Availability Suppresses Tumor Growth and Attenuates Muscle Wasting

Katrine S. Pedersen, Francesco Gatto, Bo Zerahn, Jens Nielsen, Bente K. Pedersen, Pernille Hojman, Julie Gehl

kgeh@regionsjaelland.dk

HIGHLIGHTS

Reduced access to glutamine inhibits cancer growth in vitro and in vivo

Acute exercise reduces serum glutamine

Wheel running prevents muscular changes in glutamine transport and catabolic signaling

Wheel running reduces tumor growth and tumor-induced weight loss

Article

Exercise-Mediated Lowering of Glutamine Availability Suppresses Tumor Growth and Attenuates Muscle Wasting

Katrine S. Pedersen,[1] Francesco Gatto,[2,7] Bo Zerahn,[3] Jens Nielsen,[2] Bente K. Pedersen,[1] Pernille Hojman,[1] and Julie Gehl[4,5,6,8,*]

SUMMARY

Glutamine is a central nutrient for many cancers, contributing to the generation of building blocks and energy-promoting signaling necessary for neoplastic proliferation. In this study, we hypothesized that lowering systemic glutamine levels by exercise may starve tumors, thereby contributing to the inhibitory effect of exercise on tumor growth. We demonstrate that limiting glutamine availability, either pharmacologically or physiologically by voluntary wheel running, significantly attenuated the growth of two syngeneic murine tumor models of breast cancer and lung cancer, respectively, and decreased markers of atrophic signaling in muscles from tumor-bearing mice. In continuation, wheel running completely abolished tumor-induced loss of weight and lean body mass, independently of the effect of wheel running on tumor growth. Moreover, wheel running abolished tumor-induced upregulation of muscular glutamine transporters and myostatin signaling. In conclusion, our data suggest that voluntary wheel running preserves muscle mass by counteracting muscular glutamine release and tumor-induced atrophic signaling.

INTRODUCTION

Tumors are avid glutamine consumers, and the versatile functions of glutamine within the cell make it a central nutrient for many cancers. After import, glutamine can donate its carbons for synthesis of amino acids and fatty acids and its nitrogen to synthesis of nucleotides, thereby directly supporting the accumulation of cellular building blocks (Altman et al., 2016; DeBerardinis and Cheng, 2010; Hensley et al., 2013). Glutamine also supports the generation of cellular energy, as it can be metabolized via glutamate to α-ketoglutarate, providing substrates for the citric acid cycle and ATP formation (Altman et al., 2016; DeBerardinis and Cheng, 2010). Furthermore, glutamine regulates cell signaling, as it can be rapidly exported out of the cell in exchange for essential amino acids that directly activate mTOR, thereby inducing protein translation and cell growth (Altman et al., 2016; DeBerardinis and Cheng, 2010; Hensley et al., 2013).

The pleiotropic role of glutamine in cancer cells has made glutamine uptake and metabolism attractive therapeutic targets, and several pharmacological approaches to limiting glutamine uptake and metabolism in tumor cells have been undertaken. Inhibition of the glutamine transporters SLC1A5 (Chiu et al., 2017; Schulte et al., 2018) and SLC7A5 (Häfliger et al., 2018) and various steps in glutaminolysis (glutaminase (Gross et al., 2014), aminotransferases (Korangath et al., 2015) as well as glutamate dehydrogenase (Jin et al., 2015)) have all displayed anti-tumor activity in preclinical models. These approaches share a tumor-centric methodology, interfering at the level of the tumor cell.

Glutamine is the most abundant amino acid in the circulation, constituting around 20% of the free amino acid pool (Altman et al., 2016). More than 70% of the circulating glutamine derives from skeletal muscle (Nurjhan et al., 1995) where it is either released from proteins by proteolysis or through de novo synthesis by glutamine synthetase (GS) (Felig et al., 1973; Garber et al., 1976; Kuhn et al., 1999; Schrock et al., 1980). Other tissues such as lung (Plumley et al., 1990), liver (Souba et al., 1988), and adipose tissue (Patterson et al., 2002) also have the capacity for glutamine release, yet their contributions to the plasma glutamine pool are under normal conditions modest. The majority of glutamine consumed in the diet is retained by cells in the intestinal mucosa and does not reach the circulation (Biolo et al., 1995; Wu, 1998). Thus, release from skeletal muscle is the primary source of glutamine in serum.

Exercise has the potential to regulate serum glutamine levels, yet the effect depends on the intensity and duration of the exercise intervention. Acute exercise and mild/moderate exercise interventions have yielded varying results, whereas substantial documentation exists for reduced serum glutamine levels after prolonged or strenuous exercise (Agostini and Biolo, 2010; Castell and Newsholme, 1998; Henriksson, 1991; Keast et al., 1995). The mechanism behind this observation is not completely understood but could be explained by reduced glutamine synthesis in the muscle, reduced glutamine release from muscle, or by increased glutamine uptake by other tissues (dos Santos et al., 2009).

During the 90s, it was hypothesized that exercise-induced lowering of plasma-glutamine could explain post-exercise immune changes (Newsholme and Calder, 1997). Glutamine intervention studies did, however, not restore exercise-induced immune perturbations (Hiscock and Pedersen, 2002). Here, we suggest that glutamine may represent a possible link between exercise and cancer. By lowering serum glutamine, exercise might represent a non-pharmacological approach to limiting the access of tumor cells to an important nutrient.

In this study, we hypothesized that lowering serum glutamine levels by exercise might starve tumors of glutamine, thereby contributing to the inhibitory effect of exercise on tumor growth.

RESULTS

Systemic Glutamine Availability Controls Tumor Growth

To investigate the importance of circulating glutamine levels for tumor growth, we limited the access of tumors to glutamine by treating tumor-bearing mice with methionine sulfoximine (MSO), a pharmacological inhibitor of glutamine synthetase (GS). We used two different syngeneic murine cancer models, Lewis lung carcinoma (LLC) and triple-negative breast cancer (E0771), which both harbor mutations in Kras (Agalioti et al., 2017; Yang et al., 2017) known to be associated with glutamine dependence (Gaglio et al., 2011), and which both showed markedly reduced cell proliferation when cultured in medium lacking glutamine (Figures 1A and 1F). In the tumor-bearing mice, MSO administration significantly lowered serum glutamine levels in mice with both tumor types (LLC: −57%, $p < 0.001$, Figure 1B; and E0771: −48%, $p < 0.001$, Figure 1G) and inhibited tumor growth as quantified by both tumor weight (LLC:−58%, $p < 0.01$, Figure 1C; and E0771:−34%, $p = 0.11$, Figure 1H) and tumor volume (LLC:−62%, $p < 0.01$, Figure 1D; and E0771:−44%, $p = 0.056$, Figure 1I). For both tumor types, serum glutamine concentration significantly correlated with tumor weight (Figures 1E and 1J).

MSO Treatment Regulates Glutamine Metabolism and Atrophic Signaling

LLC-tumor-bearing mice treated with MSO exhibited a significant intratumoral upregulation of the expression of glutamine transporters SLC1A5 (+83%, $p < 0.001$) and SLC7A5 (3-fold, $p < 0.001$) (Figure 2A), suggesting that these tumors attempt to maintain sufficient glutamine supply by increasing the number of transporters once serum glutamine levels become scarce. Of note, GS expression was not induced by MSO, suggesting that these tumors rely heavily on external glutamine supply. In tibialis anterior muscle of the same mice, MSO treatment strongly upregulated GS (+82%, $p < 0.01$) and the glutamine transporters SLC1A5 (+56%, $p < 0.01$) and SLC38A3 (+53%, $p < 0.001$) (Figure 2B), reflecting a compensation for the inhibition of GS activity. Interestingly, blocking glutamine synthesis also resulted in reduced intramuscular expression of the atrophy marker atrogin-1 (−44%, $p < 0.001$) (Figure 2C) and activin signaling, i.e. activin receptor 2A (AR2A) (−12%, $p < 0.001$) and activin receptor 2B (AR2B) (−39%, $p < 0.001$) (Figure 2D), suggesting a link between glutamine metabolism and muscle wasting/maintenance. However, we did not detect any tumor-induced weight loss in this experiment (Figure 2E).

Acute and Long-Term Exercise Training Regulates Glutamine Availability and Metabolism

A physiological way to reduce circulating glutamine levels is through exercise. In accordance, we found that 45 min of swimming in untrained and exercise-trained (access to running wheels for four weeks) tumor-free C57BL/6 mice induced an acute drop (−27% for untrained mice, $p < 0.01$, and −39% for trained mice, $p < 0.001$) in serum glutamine concentration, which persisted at least 2 h after the intervention (Figure 3A). Similarly, mice with E0771 tumors exhibited reduced serum glutamine concentration (−27%, $p < 0.001$) 2 h after a 45 min swimming intervention compared with a group of tumor-bearing control mice that did not swim (Figure 3B). Serum glutamine levels in mice sampled 24 and 48 h after swimming did not differ from the control group.

Lewis Lung Carcinoma
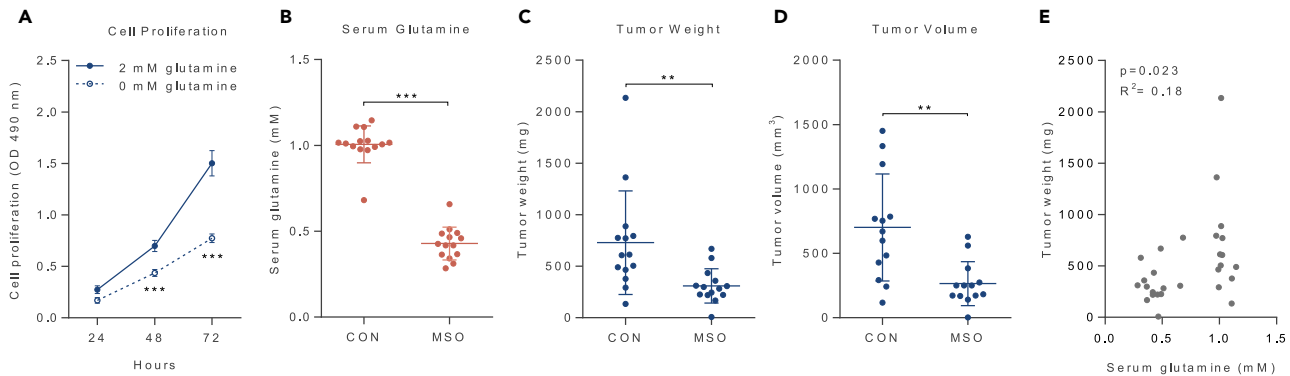
Triple negative breast cancer (E0771)
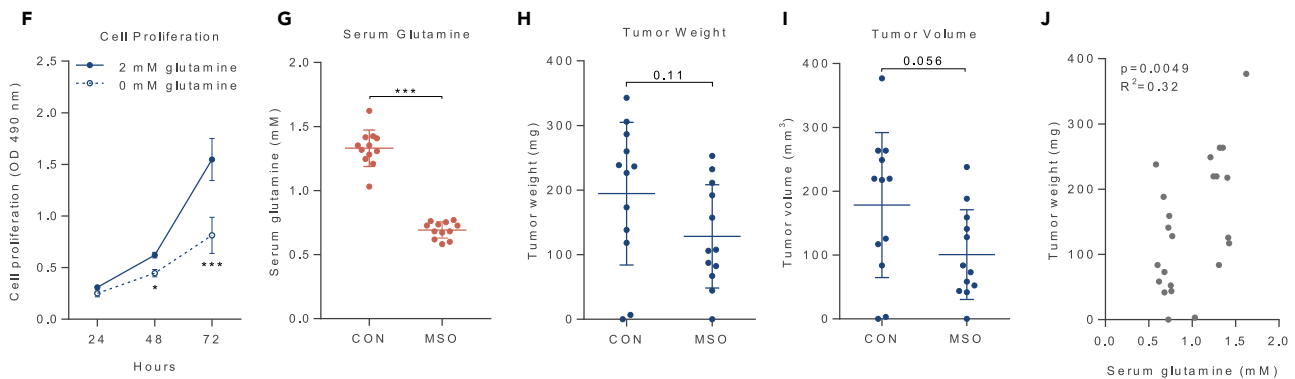
Figure 1. Reduced Access to Glutamine Inhibits Cancer Growth In Vitro and In Vivo

Cell proliferation of murine lung cancer (Lewis Lung carcinoma [LLC]) (A) and breast cancer (E0771) (F) cells in growth medium with and without glutamine. Data represent absorbance at 490 nm after an MTS assay. Serum glutamine levels in mice with LLC tumors with and without MSO treatment (B) (CON = 14, MSO = 14, unpaired Student's t-test). Size at takedown (tumor growth for 16 days) of LLC tumors from mice with and without MSO treatment quantified by weight (C) and volume (D) (CON = 14, MSO = 14, unpaired Student's t-tests). Pearson correlation (E) of LLC tumor weight and serum glutamine levels. Serum glutamine levels in mice with breast cancer (E0771) tumors with and without MSO treatment (G) (CON = 12, MSO = 12, unpaired Student's t-test). Size at takedown (tumor growth for 16 days) of E0771 tumors from mice with and without MSO treatment quantified by weight (H) and volume (I) (CON = 12, MSO = 12, unpaired Student's t-tests). Pearson correlation (J) of breast cancer (E0771) tumor weight and serum glutamine levels. Data are depicted as means +/− SD. *$p < 0.05$, **$p < 0.01$, ***$p < 0.001$.

Next, we evaluated how acute exercise could regulate intramuscular and intratumoral glutamine synthesis and transport. In mice with E0771 tumors, the reduction in serum glutamine 2 h after swimming coincided with increased intramuscular expression of GS (+45%, $p < 0.01$), SLC7A5 (4-fold, $p < 0.001$) and SLC38A3 (+21%, $p < 0.05$) (Figure 3C). In mice sampled after 24 h, SLC38A3 expression was significantly reduced (−20%, $p < 0.05$) compared with controls, whereas GS, SLC1A5, and SLC7A5 were not significantly altered (Figure 3C). In tumors from these mice, we observed modest regulation of the expression of GS (+17%, $p < 0.05$) and SLC7A5 (+17%, $p < 0.05$) 2 h after the swimming intervention, whereas SLC1A5 and SLC38A3 did not differ from control levels (Figure 3D). After 24 and 48 h no differences were detected (Figure 3D). This suggests that acute exercise directly impacts glutamine synthesis and transport in tumor and muscle tissue with roughly the same pattern but to a larger extent in the muscles.

We went on to investigate the effect of long-term training. C57BL/6 mice were randomized to cages with and without running wheels for four weeks and subsequently inoculated with E0771 tumors. Voluntary wheel running significantly reduced tumor growth compared with control mice as quantified by tumor weight (−43%, $p < 0.01$, Figure 3E) and tumor volume (−42%, $p < 0.01$, Figure 3F). Serum glutamine levels obtained at termination of the experiment did not differ between control and wheel running mice
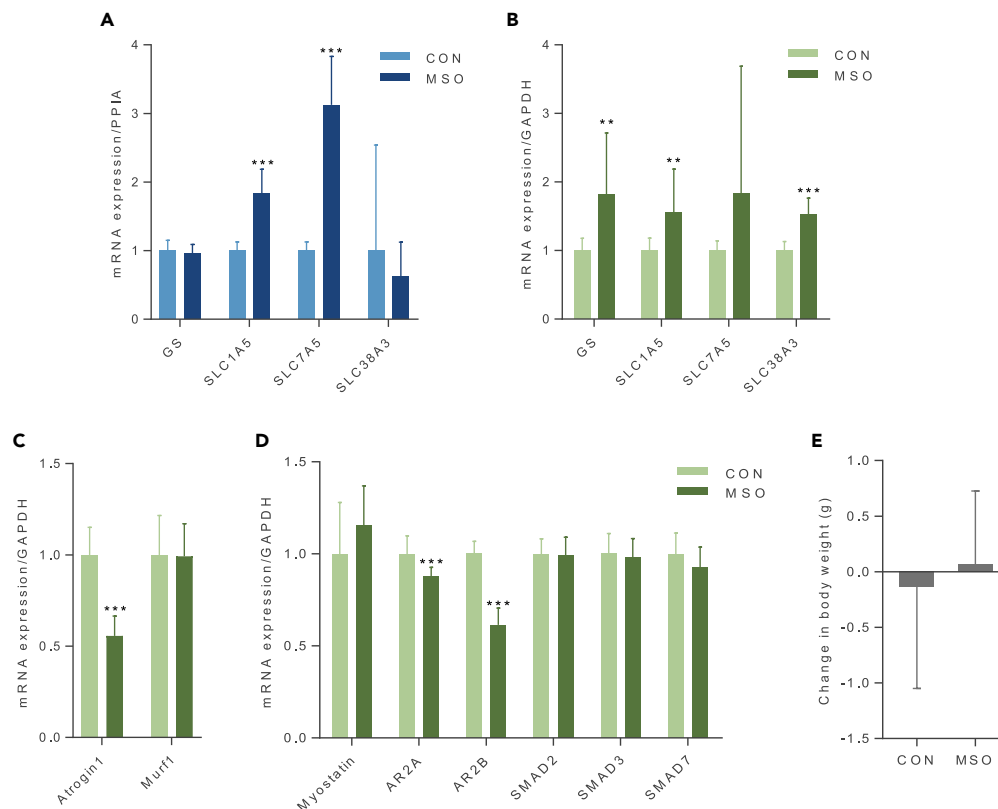
Figure 2. Blocking GS Activity Affects Glutamine Metabolism and Transport and Atrophic Signaling in Tumors and Muscle

Expression of genes involved in glutamine transport and metabolism in LLC tumors from mice with and without MSO treatment (A) (CON = 13, MSO = 13, unpaired Student's t-tests). Gene expression of glutamine synthetase (GS) and glutamine transporters (B), atrophy markers (C), and myostatin signaling cascade (D) in tibialis anterior muscle from mice with LLC tumors with and without MSO treatment (CON = 13, MSO = 13, unpaired Student's t-tests). Change in body weight (excluding tumor weight) in the period of tumor challenge (tumor growth for 16 days) in mice with LLC tumors with and without MSO treatment (E) (CON = 14, MSO = 14, paired Student's t-tests of weight at tumor induction and takedown). Data are depicted as means +SD. *p < 0.05, **p < 0.01, ***p < 0.001.

(Figure 3G). Muscles from wheel-running mice had significantly reduced expression of GS (−46%, p < 0.001) and the glutamine transporters SLC1A5 (−29%, p < 0.001) and SLC38A3 (−41%, p < 0.001) (Figure 3H) compared with controls, suggesting that exercise resulted in a long-term adaptive suppression of the expression of GS and glutamine transporters in muscles.

Voluntary Wheel Running Prevents Tumor-Induced Weight Loss

Next, we set out to investigate muscle maintenance in a cachexia-inducing tumor type. C57BL/6 mice were randomized to cages with and without running wheels, and after four weeks inoculated with LLC cells. Wheel running significantly reduced tumor growth in this tumor model as quantified by both tumor weight (−90%, p < 0.01, Figure 4A) and tumor volume (−91%, p < 0.01, Figure 4B). In order to shed light on the pronounced tumor growth suppression in this mouse model, we opted to perform RNA sequencing to elucidate genome-wide regulation in the tumors. RNA sequencing of LLC tumor tissue revealed virtually no differential regulation of intratumoral gene expression between tumors from the control and exercise groups as evidenced by principal component analyses (Figures 4C and S1 and Table S1). Accordingly, targeted PCR against glutamine transporters found no significant differences in the expression patterns in LLC tumors in response to voluntary wheel running (Figure 4D).

The LLC-tumor-bearing mice exhibited a significant weight loss in the period of tumor burden (−1.14 g, p < 0.01), which was completely prevented by wheel running (p < 0.01 for interaction in a two-way ANOVA) (Figure 4E). The increase in lean body mass in the period of tumor burden observed across the
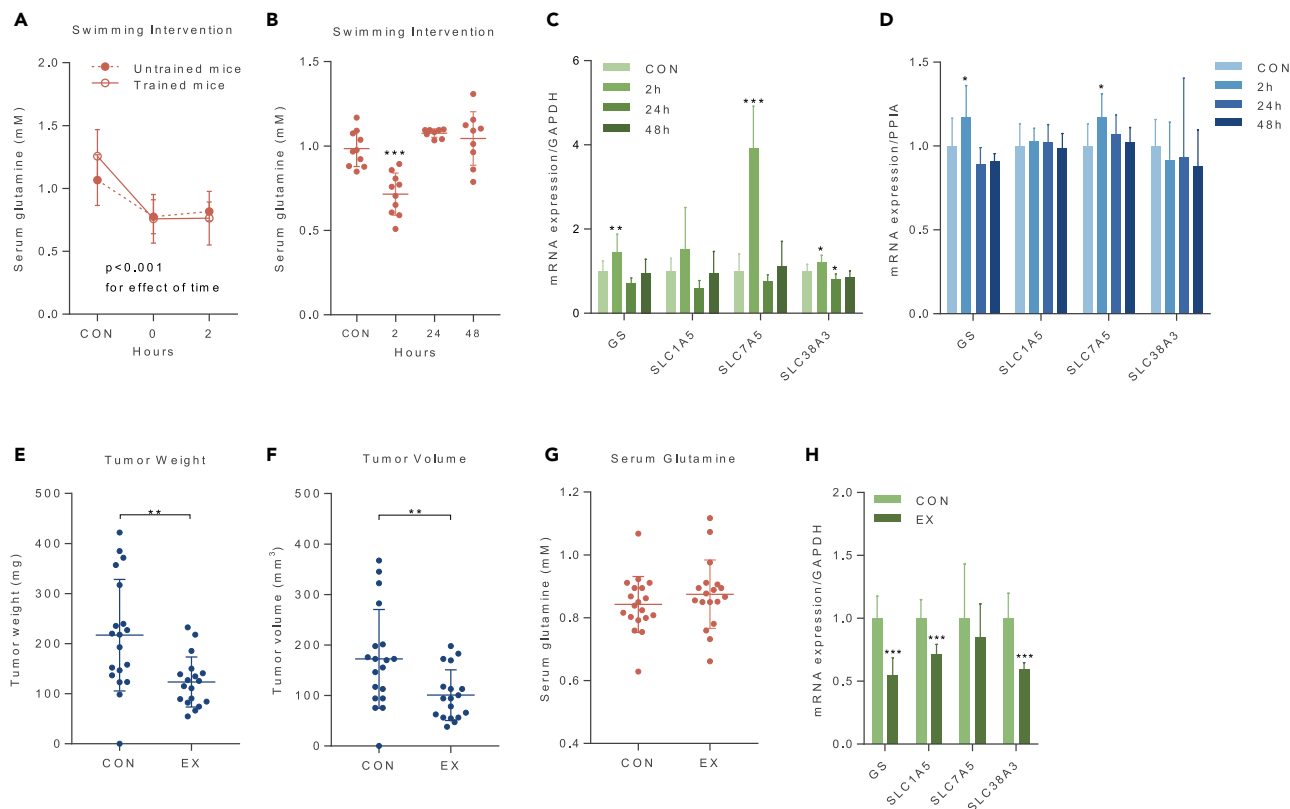
Figure 3. Acute Swimming Reduces Serum Glutamine and Voluntary Wheel Running Reduces Tumor Growth and Affects Glutamine Synthesis and Transport in Muscle and Tumor

Serum glutamine levels (A) from trained and untrained mice (+/− 4 weeks of voluntary wheel running) sampled before (CON), immediately after (0), and 2 h into the recovery (2) of a 45-min swimming intervention (untrained = 9, trained = 7, two-way ANOVA with repeated measures, Bonferroni correction). Serum glutamine levels (B) from four groups of mice with E0771 tumors, taken down at the indicated time points after a 45-min swimming intervention (CON = 9, 2 h = 10, 24 h = 10, 48 h = 9, one-way ANOVA with Bonferroni correction). Gene expression of GS and glutamine transporters (C) in tibialis anterior muscle from mice in (B) (one-way ANOVA with Bonferroni correction). Gene expression of GS and glutamine transporters (D) in E0771 tumors from the same mice as in (B) (one-way ANOVA with Bonferroni correction). Size at takedown (tumor growth for 15 days) of E0771 tumors quantified by weight (E) and volume (F) from sedentary (CON) and wheel running (EX) C57BL/6 mice (CON = 18, EX = 18, unpaired Student's t-tests). Serum glutamine levels (G) in mice from E and F (CON = 18, EX = 18, unpaired Student's t-tests). Gene expression of GS and glutamine transporters (H) in tibialis anterior muscle from mice in E and F (CON = 16, EX = 14, unpaired Student's t-tests). Data are depicted as means +/− SD, *$p < 0.05$, **$p < 0.01$, ***$p < 0.001$.

study in control mice tended to be attenuated in LLC-tumor-bearing mice ($p = 0.087$), whereas it was normalized by wheel running (Figure 4F). Tumor-free mice exhibited reductions in fat mass but in the same period an increase in lean body mass (Figure 4G).

When exploring the muscular signaling in these mice, we found that LLC tumors induced the mRNA expression of SLC7A5 (+57%, $p < 0.01$) and tended to induce the expression of SLC1A5 (+16%, $p = 0.093$) (Figure 4I). This induction of glutamine transporters by LLC tumors was abolished by wheel running (Figure 4I). In continuation, the presence of LLC tumors induced the expression of the atrophy markers atrogin-1 (+50%, $p < 0.05$) and MuRF1 (+63%, $p < 0.05$) (Figure 4J) and myostatin signaling (myostatin: +57%, $p < 0.001$, activin receptor 2A: +26%, $p < 0.001$, and SMAD3: +73%, $p < 0.001$) (Figure 4H). These inductions were completely abolished with wheel running (Figures 4H and 4J), consistent with the observed weight loss and impaired gain of lean mass. No statistically significant differences were observed in the muscular protein expression of GS, the glutamine transporter SLC38A3, or the atrophy markers atrogin-1 and Murf1 (Figure 4K).

Wheel Running Prevents Tumor-Induced Weight Loss Independently of Tumor Size

Because wheel running had a marked effect on tumor growth, we confirmed the effect of voluntary wheel running on tumor-induced weight loss and intramuscular signaling in a separate experiment where
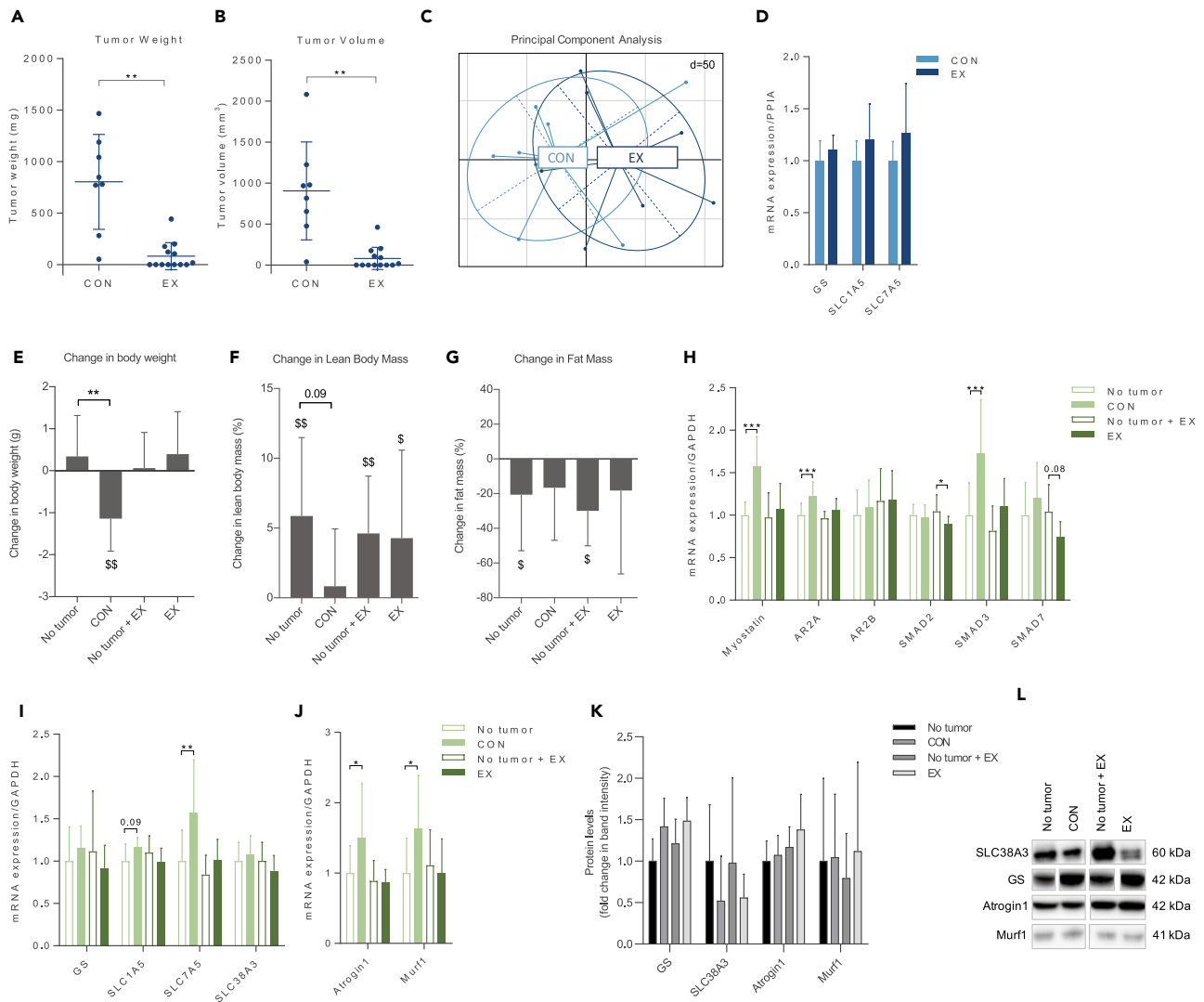
Figure 4. Voluntary Wheel Running Reduces Tumor Growth and Prevents Tumor-Induced Weight Loss and Intramuscular Changes in Glutamine Transport and Catabolic Signaling

Size at takedown (tumor growth for 23 days) of LLC tumors quantified by weight (A) and volume (B) from sedentary and wheel running C57BL/6 mice (CON = 8, EX = 13, unpaired Student's t-tests). Principal Component Analysis of intratumoral gene expression profiles (C) obtained by RNA-sequencing of tumors in (A and B) (see also Figure S1 and Table S1). Gene expression of GS and glutamine transporters (D) in tumors in (A and B). Change in body weight in the period of tumor challenge (tumor growth for 23 days) (E) in sedentary and wheel-running C57BL/6 mice with and without LLC tumors (no tumor = 12, CON = 8, no tumor + EX = 10, EX = 13, two-way ANOVA with Bonferroni correction, p = 0.003 for interaction. $ indicates a statistically significant weight change in a paired Student's t-test of weight at tumor induction and takedown). Percentage change in lean body mass (F) and fat mass (G) during tumor challenge obtained by DXA scanning of mice from Figure E prior to tumor induction and at takedown (tumor growth for 23 days) (two-way ANOVA with Bonferroni correction. $ indicates a statistically significant change in lean body mass and fat mass in a paired Student's t-test of lean and fat mass at tumor induction and takedown). Gene expression of myostatin signaling cascade (H), GS, and glutamine transporters (I) and atrophy markers (J) in tibialis anterior muscle of mice from (E) (two-way ANOVA with Bonferroni correction, p-values for interaction: myostatin = 0.0096, SMAD3 = 0.092, SMAD7 = 0.019, SLC1A5 = 0.017, atrogin-1 = 0.058, MuRF1 = 0.042). Protein expression of GS, glutamine transporters, and atrophy markers (K) in gastrocnemius muscle of mice from (E). Data represent fold changes in Western blot band intensity. The signal for the protein of interest in each lane was normalized to the total protein amount in the same lane. Data represent the mean of two independent experiments (two-way ANOVA with Bonferroni correction). Representative Western blot images (L) of GS, glutamine transporters, and atrophy markers quantified in (K). Data are depicted as mean ± SD. *p < 0.05, **p < 0.01, ***p < 0.001, $ p < 0.05, $$ p < 0.01.

the mice were euthanized when tumor volume was estimated to 1 cm³ by external calipers, yielding two groups of mice with the same average tumor size (Figures 5A and 5B). In line with the previous experiment, LLC tumors induced a significant weight loss of −1.13 g (p < 0.01), which was completely abolished by voluntary wheel running (Figure 5C), despite similar tumor burden in the control and exercise groups. In
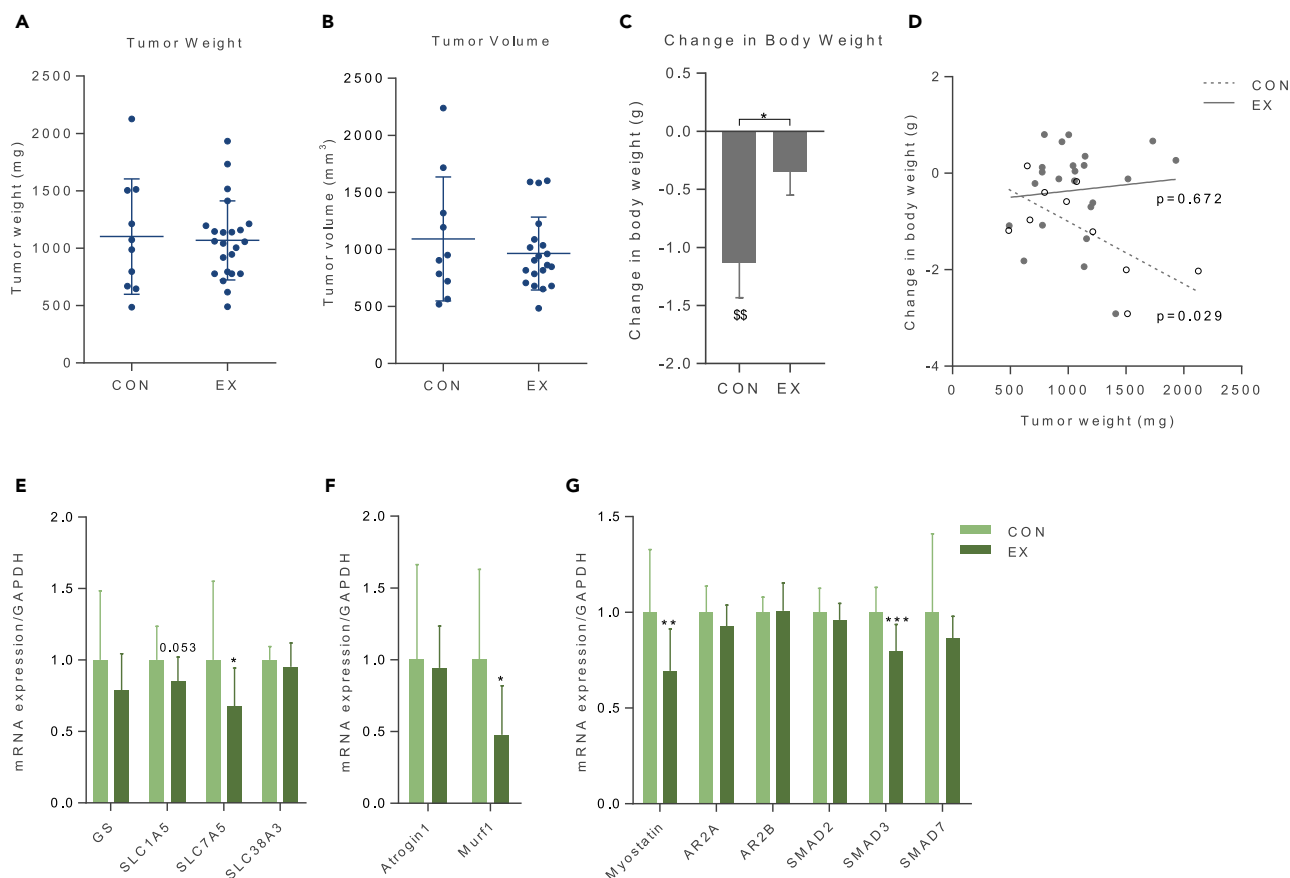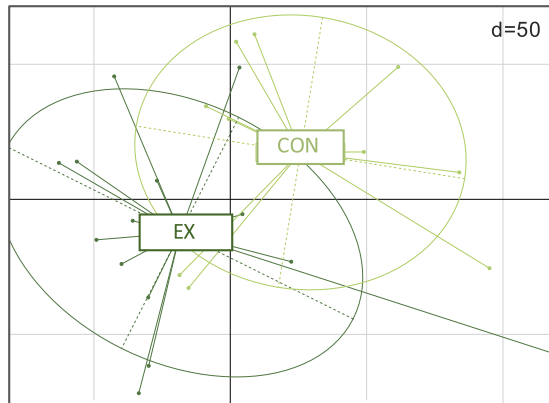
Figure 5. Voluntary Wheel Running Prevents Tumor-Induced Weight Loss and Regulates Intramuscular Signaling Independently of Tumor Size

Size at takedown of LLC tumors quantified by weight (A) and volume (B) from sedentary and wheel running C57BL/6 mice (CON = 10, EX = 23, unpaired Student's t-tests) (mean period of tumor growth: CON = 23.3 days +/− 4.09, EX = 23.5 days +/−4.9). Change in body weight in the period of tumor challenge (excluding tumor weight) (C) in mice from (A and B) (CON = 10, EX = 23, unpaired Student's t-test. $ indicates a statistically significant weight change in a paired Student's t-test of weight at tumor induction and takedown). Linear regression (D) of tumor weight versus change in body weight in mice from (A and B). Gene expression of GS and glutamine transporters (E), atrophy markers (F), and myostatin signaling cascade (G) in tibialis anterior muscle from mice in (A and B) (CON = 10, EX = 21, unpaired student's t test). Data are depicted as mean ± SD. *p < 0.05, **p < 0.01, ***p < 0.001, $ p < 0.05, $$ p < 0.01.

the control group, tumor size correlated with the observed weight loss (p < 0.05) (Figure 5D), whereas this correlation was abolished in the wheel running group. As before, the intramuscular expression levels of glutamine transporters SLC1A5 (−15%, p = 0.053) and SLC7A5 (−32%, p < 0.05) (Figure 5E), as well as the atrophy marker MuRF1 (−52%, p < 0.05) (Figure 5F) and myostatin signaling (myostatin: −31%, p < 0.01, and SMAD3:−20%, p < 0.01) (Figure 5G) were reduced by wheel running, suggesting that the regulation by wheel running can overcome the tumor-induced changes independently of tumor size.

Global Gene Expression in Muscles

Given the protection against tumor-induced weight loss by wheel running, we explored intramuscular exercise adaptations in response to voluntary wheel running. RNA sequencing of muscle tissue from the mice with similarly sized LLC tumors showed significant changes in the muscular transcription of 265 genes and a clear separation between the control and exercise groups by principal component analysis (Figures 6A and S2 and Table S2). Subsequent pathway analysis revealed that the upregulated genes were mostly associated to myogenesis and oxidative phosphorylation (Figure 6B), demonstrating that mice with access to running wheels exhibited classical intramuscular exercise adaptations despite LLC tumor burden. Interestingly, genes related to alternative splicing were also identified in the pathway analysis (Figure 6C). In support of these findings, we measured the splice variants of PGC-1α, which demonstrated differential expression with wheel running and tumor burden (Figure 6D).

A

Principal Component Analysis

d=50

CON

EX

B

Hallmark Pathway Analysis

2	19.5	46	MYC TARGETS
1	6.5	47	HEME METABOLISM
11	12	40	HEDGEHOG SIGNALING
24	13	21	IL2 STAT5 SIGNALING
3	45	49	G2M CHECKPOINT
46	7	5	ANGIOGENESIS
49	1	1	EPITHELIAL MESENCHYMAL TRANSITION
49	5	1	OXIDATIVE PHOSPHORYLATION
45	5	4	CHOLESTEROL HOMEOSTASIS
46	2	4	ADIPOGENESIS
44	1	1	MYOGENESIS

Distinct–directional (dn) Non–directional Distinct–directional (up)

C

KEGG Pathway Analysis

181	6.5	1	CARDIAC MUSCLE CONTRACTION
181	3	1	PARKINSON'S DISEASE
181	2.5	1	OXIDATIVE PHOSPHORYLATION
181	32.5	1	HUNTINGTON'S DISEASE
181	11.5	1	ECM RECEPTOR INTERACTIONS
181	1	1	ALZHEIMER'S DISEASE
157	3.5	26	FOCAL ADHESION
3	27.5	180	ADHERENS JUNCTION
4	26	183	VASCULAR SMOOTH MUSCLE CONTRACTION
11	7.5	169	INSULIN SIGNALING PATHWAY
1	12.5	186	SPLICEOSOME
9	1	177	CIRCADIAN RHYTHM MAMMAL

Distinct–directional (dn) Non–directional Distinct–directional (up)

D

No tumor
CON
No tumor + EX
EX

Figure 6. Voluntary Wheel Running Induces Classical Intramuscular Exercise Adaptations in Tumor-Bearing Mice

Principal component analysis of intramuscular gene expression profiles (A) obtained by RNA-sequencing of tibialis anterior muscle from mice in Figures 5A and 5B (CON = 10, EX = 14 [samples selected based on which mice ran the most]) (see also Figure S2 and Table S2). Heatmaps of ranks for hallmark (B) and Kyoto Encyclopedia of Genes and Genomes (KEGG) (C) gene-sets associated with genes significantly downregulated (left column), upregulated (right column), or regulated independently of direction (middle column) in muscle tissues from mice in Figures 5A and 5B. Only the 11 top ranked (most regulated) gene-sets are shown (out of 50 for hallmarks pathways, out of 186 for KEGG). The more red the color, the higher the rank. Gene expression of PGC-1α splice variants (D) in tibialis anterior muscle from mice in Figure 5E; n.d., not detectable. Data are depicted as mean +SD. *p < 0.05, **p < 0.01, ***p < 0.001.
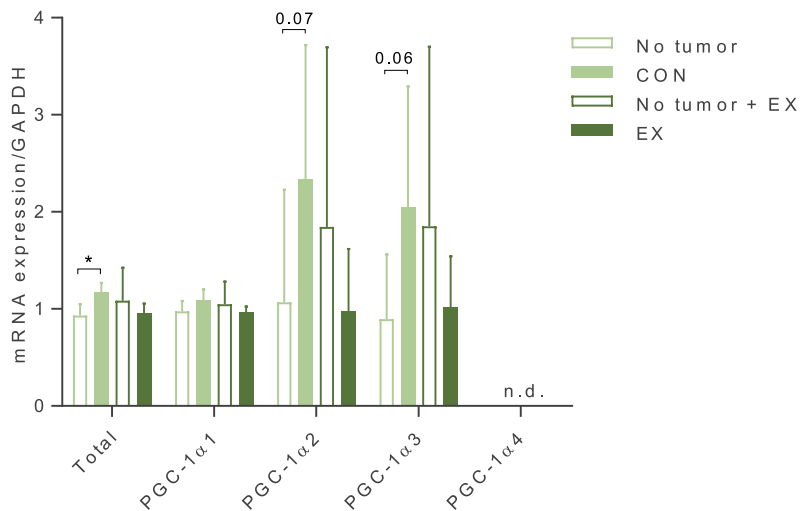
Co-regulation of Glutamine and Myostatin in Muscle Cells

Across the murine studies, we observed concurrent regulation of glutamine metabolism and myostatin/atrophy signaling. Thus, to explore any co-regulation we investigated the effect of myostatin stimulation and reduced glutamine availability on the expression of glutamine transporters in C2C12 myotubes. In accordance with others (Zhang et al., 2017) we found that differentiation of C2C12 myotubes in medium conditioned by cultured LLC cells yielded visibly thinner myotubes compared with C2C12 grown under control conditions (Figure 7A). To investigate if tumor-derived myostatin might be responsible for the tumor-induced expression of glutamine transporters in muscle observed in the murine studies, we stimulated fully differentiated C2C12 myotubes with recombinant myostatin (400 ng/mL) for 2.5 h. Myostatin reduced the expression of GS (−15%, p < 0.001), SLC1A5 (−7%, p = 0.07), and SLC7A5 (−9%, p < 0.01) (Figure 7B), suggesting that the tumor-induced upregulation of glutamine transporters in muscle is not driven by myostatin.

Next, we exposed fully differentiated C2C12 myotubes to reduced glutamine availability in the cell medium. Compared with standard cell medium conditions (3.9 mM glutamine), 2.5 h of incubation in medium with 0.5 mM glutamine reduced the expression levels of GS (−9%, p < 0.01), SLC1A5 (−17%, p < 0.001), and SLC7A5 (−33%, p < 0.001) (Figure 7C), whereas complete glutamine depletion for 2.5 h reduced the expression of GS (−10%) and induced the expression of SLC1A5 (+32%, p < 0.001) and SLC7A5 (57%, p < 0.001) (Figure 7C). This suggests that external glutamine availability regulates the expression of glutamine transporters in myotubes. Incubation of C2C12 cells in medium with 0.5 mM glutamine did not significantly affect the expression of atrophy markers (Figure 7D) or myostatin (Figure 7E) but reduced the expression of activin receptor 2A (−8%, p < 0.05), activin receptor 2B (−12%, p < 0.01), and SMAD3 (−13%, p < 0.001) (Figure 7D). Complete glutamine depletion for 2.5 h induced the expression levels of atrogin-1 (+12%, p < 0.05), tended to induce MuRF1 (+13%, p = 0.09) (Figure 7D), and induced activin receptor 2A (+8%, p < 0.05), SMAD2 (+13%, p < 0.05), and SMAD7 (+22%, p < 0.01) (Figure 7E).

DISCUSSION

Here, we demonstrate that reducing glutamine availability, through either pharmacological treatment or voluntary wheel running, significantly attenuated the growth of two different syngeneic murine tumor models, respectively the triple-negative breast cancer model E0771 and the lung cancer model LLC. Both interventions decreased intramuscular mRNA expression of atrophy markers in tumor-bearing mice, resulting in a complete prevention of LLC tumor-induced weight loss with wheel running. Thus, our studies suggest that voluntary wheel running may preserve muscle mass in mice despite a large tumor burden by counteracting atrophic signaling and muscular glutamine release.

Regulation of tumor growth by limiting glutamine utilization has previously focused on drugs targeting intratumoral metabolism. Here, we aimed to regulate glutamine availability by addressing the systemic production. MSO treatment inhibits GS activity and in our study lowered glutamine levels in serum by approximately 50%. This markedly correlated with reduced growth of the two investigated tumor models, underscoring that tumor growth might be controlled by reducing glutamine availability. As a consequence, we observed that LLC tumors upregulated SLC1A5 and SLC7A5 expression. These two glutamine transporters are believed to be functionally coupled in tumors ensuring both glutamine import for intracellular glutaminolysis and export in exchange for essential amino acids and activation of cell growth via mTOR (Bhutia and Ganapathy, 2016). Upregulation of this transport system by MSO likely reflects a compensatory response by tumors to the reduced glutamine availability. In muscle tissue from LLC-tumor-bearing mice, we observed a significant reduced expression of the atrophy marker atrogin-1 and activin receptor 2A and 2B after MSO treatment, suggesting a link between glutamine metabolism and muscle wasting/maintenance.
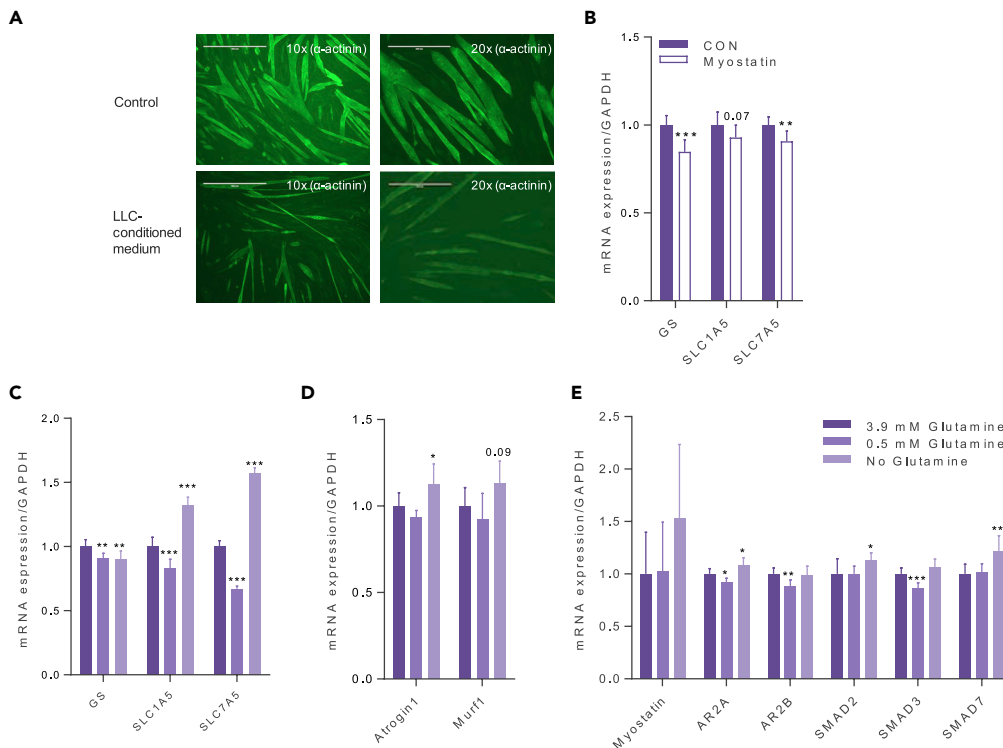
Figure 7. Co-regulation of Glutamine and Myostatin

Representative pictures of C2C12 myotubes differentiated under control conditions or in 25% medium conditioned by LLC cells, stained for α-actinin (A). Gene expression of GS and glutamine transporters (B) in fully differentiated C2C12 myotubes after 2.5 h incubation with or without myostatin (400 ng/mL) (n = 8, unpaired Student's t-test). Gene expression of GS and glutamine transporters (C), atrophy markers (D), and myostatin signaling cascade (E) in fully differentiated C2C12 myotubes after 2.5 h incubation in medium containing the indicated concentrations of glutamine (n = 8, 1-Way ANOVA with Bonferroni correction). Data are depicted as mean +SD. *p < 0.05, **p < 0.01, ***p < 0.001.

Like MSO treatment, acute exercise, in the form of a 45-min swimming intervention, significantly reduced glutamine levels in serum in both tumor-free and E0771 tumor-bearing mice. The reduction in serum glutamine of about 30%–40% persisted at least 2 h into the recovery period and was restored to baseline levels after 24 h. Acute, transient changes in systemic factors, such as catecholamines and myokines, accompanying an acute exercise bout have previously been linked to the anti-cancer effect of exercise (Dethlefsen et al., 2017). Our current paper suggests the addition of glutamine to the list of factors altered by acute exercise, which collectively contribute to an environment unfavorable to cancer growth and progression. In parallel, we found that swimming increased the expression of GS and glutamine transporters in muscle, whereas regulation in the tumor was less affected by exercise training. In continuation, we found that long-term training in the form of voluntary wheel running significantly reduced the growth of both LLC and E0771 tumors, and as after the acute swimming intervention, we hardly observed any differential gene expression in the tumors, wherease transcriptional adaptations did occur in muscle tissue.

Mice with E0771 tumors exhibited significantly reduced intramuscular expression of GS and glutamine transporters in response to voluntary wheel running, indicative of a long-term adaptive suppression of muscular expression of GS and glutamine transporters by exercise.

In muscle tissue, LLC tumors induced the mRNA expression of several components of the atrophic signaling cascade, as has been previously described (Busquets et al., 2012). Voluntary wheel running completely prevented this tumor-induced expression, in a pattern similar to the effect of MSO. Inhibition of myostatin signaling has in several mouse studies been shown to prevent tumor-induced cachexia and prolong survival (Busquets et al., 2012; Zhou et al., 2010). Our findings are in full accordance with this and extend these previous findings by suggesting that the abolishment of tumor-induced mRNA expression of atrophy/myostatin in muscle tissue can be obtained by voluntary wheel running, resulting

in prevention of tumor-induced weight loss. We did, however, not observe changes in the expression of atrophic markers on the protein level. In addition to the induced mRNA expression of atrophic markers, we observed an increased mRNA expression of the glutamine exporter SLC7A5 in the presence of LLC tumors (Baird et al., 2009; Hodson et al., 2018). Considering the dependence of LLC tumors on external glutamine supply, this might suggest that LLC tumors are able to directly influence glutamine export from skeletal muscle. It is generally accepted that cachexia-inducing tumors can reprogram the host metabolism in a manner that favors nutrient supply to the tumor at the expense of host tissue wasting (Busquets et al., 2014; Porporato, 2016). Several tumor models have previously been documented to affect muscle glutamine synthesis and transport. In rats carrying methylcholanthrene-induced (MCA) fibrosarcoma, muscular GS activity and expression was increased, glutamine release from muscle increased, and intramuscular glutamine concentration was reduced (Chen et al., 1993). Likewise, in rats carrying Walker 256 carcinosarcoma, skeletal muscle and plasma glutamine content decreased and release of glutamine from extensor digitorumlongus (EDL) muscle increased (Parry-Billings et al., 1991). A recent tracer-experiment in mice revealed incorporation of muscle-derived glutamine into subcutaneous C26 tumors, possibly directly recruited by tumor-derived high-mobility group box 1 (HMGB1) protein release to the circulation (Luo et al., 2014). Our experiments suggest that voluntary wheel running can counteract this tumor-induced regulation of glutamine export from skeletal muscle. Glutamine is the most abundant free amino acid in muscle tissue, estimated to make up more than 40% of the free intramuscular amino acid pool (Bergström et al., 1974; Löfberg et al., 2002). Additionally, it is incorporated into proteins, where it may account for between 4% and 14% of intact muscle protein depending on the mode of estimation (Darmaun et al., 1988; Kuhn et al., 1999). Assuming that LLC tumors can increase glutamine release from skeletal muscle, usurping muscular glutamine could be one mechanism by which LLC tumors induce muscle wasting, simply by depleting the large intramuscular glutamine pool.

The proposition that an effect of exercise could be to starve tumors of a key factor for growth goes well with recent epidemiological data showing that exercise lowers the risk of cancer across histologies (Moore et al., 2016). Also, in our study a prominent tumor inhibitory effect was found in two rather different tumor models, namely a lung cancer model and a triple-negative breast cancer model, in line with glutamine being important in tumor growth across histologies (Chiu et al., 2017; Gross et al., 2014; Häfliger et al., 2018; Schulte et al., 2018). Recent evidence points to a number of effects of exercise that lead to tumor growth inhibition, as reviewed previously (Hojman et al., 2018), and the current paper adds to the list of factors that may explain the rather striking findings placing exercise as central in cancer prevention.

We have previously shown that voluntary wheel running can prevent tumor growth across a panel of murine tumors. In B16 malignant melanoma tumors, we identified a marked exercise-mediated upregulation of NK-cell infiltration into tumors as an underlying mechanism for exercise-mediated suppression of tumor growth (Pedersen et al., 2016). In the present study, we did not find any exercise-induced expression of NK cell markers in LLC tumors (data not shown), underlying that exercise may influence tumor growth by different pathways dependent on tumor type.

In conclusion, we show that limiting glutamine availability, either pharmacologically or physiologically by wheel running, decreased tumor growth and reduced mRNA expression of atrophy markers in muscle from tumor-bearing mice. In continuation, we demonstrated a complete abolishment of LLC-tumor-induced weight loss by voluntary wheel running, independently of the effect of wheel running on tumor growth.

Limitations of the Study

The LLC and E0771 tumor models applied in this project constitute transplantable syngeneic tumor models. A general limitation inherent to all transplantable tumor models is the bypassing of the initial steps in tumor development during which cells are transformed and starts neoplastic division. Accordingly, in the interventions with MSO and voluntary wheel running, potential effects on initial tumor development are not investigated with this approach. Thus, the present results exclusively represent effects on already transformed tumor cells, their establishment as solid tumors, and subsequent tumor growth.

Swimming and voluntary wheel running were applied as exercise interventions, thus representing both a forced and a voluntary type. Because the swimming intervention does represent forced exercise it is likely that a stress response was evoked in the mice during the 45 min of swimming. Thus, effects of the swimming intervention cannot necessarily be attributed solely to the exercise component of the intervention. To

avoid subjecting the mice to the stress induced by single housing, mice were housed in pairs. Thus, for the voluntary wheel running intervention, the LCD Activity Wheel Counters only provide information about the daily distance covered per cage, whereas the distribution of this distance between two mice in a cage remains unknown. The average distances reported per mouse per day are thus approximations.

METHODS

All methods can be found in the accompanying Transparent Methods supplemental file.

DATA AND CODE AVAILABILITY

The accession number for the RNA-sequencing analysis of LLC tumor tissue reported in this paper is ArrayExpress: E-MTAB-5311. The accession number for the RNA-sequencing analysis of murine muscle tissue reported in this paper is ArrayExpress: E-MTAB-5974.

SUPPLEMENTAL INFORMATION

Supplemental Information can be found online at https://doi.org/10.1016/j.isci.2020.100978.

AUTHOR CONTRIBUTIONS

K.S.P. and F.G. designed and performed the experiments and analyzed the data. B.Z. assisted with performing the experiments. J.G., J.N., and B.K.P. contributed with essential ideas and discussion. P.H. designed the experiments and supervised the work. K.S.P. and P.H. wrote the manuscript. All authors have read and approved the final version of the manuscript.

DECLARATION OF INTERESTS

The authors declare no competing interests.

REFERENCES

Agalioti, T., Giannou, A.D., Krontira, A.C., Kanellakis, N.I., Kati, D., Vreka, M., Pepe, M., Spella, M., Lilis, I., Zazara, D.E., et al. (2017). Mutant KRAS promotes malignant pleural effusion formation. Nat. Commun. 8, 15205.

Agostini, F., and Biolo, G. (2010). Effect of physical activity on glutamine metabolism. Curr. Opin. Clin. Nutr. Metab. Care 13, 58–64.

Altman, B.J., Stine, Z.E., and Dang, C.V. (2016). From Krebs to clinic: glutamine metabolism to cancer therapy. Nat. Rev. Cancer 16, 619–634.

Baird, F.E., Bett, K.J., MacLean, C., Tee, A.R., Hundal, H.S., and Taylor, P.M. (2009). Tertiary active transport of amino acids reconstituted by coexpression of System A and L transporters in Xenopus oocytes. Am. J. Physiol. Metab. 297, E822–E829.

Bergström, J., Fürst, P., Norée, L.O., and Vinnars, E. (1974). Intracellular free amino acid concentration in human muscle tissue. J. Appl. Physiol. 36, 693–697.

Bhutia, Y.D., and Ganapathy, V. (2016). Glutamine transporters in mammalian cells and their functions in physiology and cancer. Biochim. Biophys. Acta 1863, 2531–2539.

Biolo, G., Fleming, R.Y., Maggi, S.P., and Wolfe, R.R. (1995). Transmembrane transport and intracellular kinetics of amino acids in human skeletal muscle. Am. J. Physiol. Metab. 268, E75–E84.

Busquets, S., Toledo, M., Orpi, M., Massa, D., Porta, M., Capdevila, E., Padilla, N., Frailis, V., Lopez-Soriano, F.J., Han, H.Q., et al. (2012). Myostatin blockage using actRIIB antagonism in mice bearing the Lewis lung carcinoma results in the improvement of muscle wasting and physical performance. J. Cachexia. Sarcopenia Muscle 3, 37–43.

Busquets, S., Stemmler, B., Argilés, J.M., and López-Soriano, F.J. (2014). Cancer cachexia: understanding the molecular basis. Nat. Rev. Cancer 14, 754–762.

Castell, L.M., and Newsholme, E.A. (1998). Glutamine and the effects of exhaustive exercise upon the immune response. Can. J. Physiol. Pharmacol. 76, 524–532.

Chen, M.K., Espat, N.J., Bland, K.I., Copeland, E.M., and Souba, W.W. (1993). Influence of progressive tumor growth on glutamine metabolism in skeletal muscle and kidney. Ann. Surg. 217, 655–666, discussion 666-7.

Chiu, M., Sabino, C., Taurino, G., Bianchi, M.G., Andreoli, R., Giuliani, N., and Bussolati, O. (2017). GPNA inhibits the sodium - independent transport system l for neutral amino acids. Amino Acids 49, 1365–1372.

Darmaun, D., Matthews, D.E., and Bier, D.M. (1988). Physiological hypercortisolemia increases proteolysis, glutamine, and alanine production. Am. J. Physiol. 255, E366–E373.

DeBerardinis, R.J., and Cheng, T. (2010). Q's next: the diverse functions of glutamine in metabolism, cell biology and cancer. Oncogene 29, 313–324.

Dethlefsen, C., Pedersen, K.S., and Hojman, P. (2017). Every exercise bout matters: linking systemic exercise responses to breast cancer control. Breast Cancer Res. Treat. 162, 399–408.

Felig, P., Wahrent, J., and Raft, L. (1973). Evidence of interorgan amino acid transport by blood cells in humans. Proc. Natl. Acad. Sci. U S A 70, 1775–1779.

Gaglio, D., Metallo, C.M., Gameiro, P.A., Hiller, K., Danna, L.S., Balestrieri, C., Alberghina, L., Stephanopoulos, G., and Chiaradonna, F. (2011). Oncogenic K-Ras decouples glucose and glutamine metabolism to support cancer cell growth. Mol. Syst. Biol. 7, 1–15.

Garber, A.J., Karl, I.E., and Kipnis, D.M. (1976). Alanine and glutamine synthesis and release from skeletal muscle. I. Glycolysis and amino acid release. J. Biol. Chem. 10, 826–835.

Gross, M.I., Demo, S.D., Dennison, J.B., Chen, L., Chernov-Rogan, T., Goyal, B., Janes, J.R., Laidig, G.J., Lewis, E.R., Li, J., et al. (2014). Antitumor activity of the glutaminase inhibitor CB-839 in triple-negative breast cancer. Mol. Cancer Ther. 13, 890–901.

Henriksson, J. (1991). Effect of exercise on amino acid concentrations in skeletal muscle and plasma. J. Exp. Biol. 160, 149–165.

Hensley, C.T., Wasti, A.T., and Deberardinis, R.J. (2013). Glutamine and cancer: cell biology , physiology , and clinical opportunities. J. Clin. Invest. 123, 3678–3684.

Hiscock, N., and Pedersen, B.K. (2002). Exercise-induced immunodepression- plasma glutamine is not the link. J. Appl. Physiol. 93, 813–822.

Hodson, N., Brown, T., Joanisse, S., Aguirre, N., West, D.W.D., Moore, D.R., Baar, K., Breen, L., and Philp, A. (2018). Characterisation of L-type amino acid transporter 1 (LAT1) expression in human skeletal muscle by immunofluorescent microscopy. Nutrients 10, E23.

Hojman, P., Gehl, J., Christensen, J.F., and Pedersen, B.K. (2018). Molecular mechanisms linking exercise to cancer prevention and treatment. Cell Metab. 27, 10–21.

Häfliger, P., Graff, J., Rubin, M., Stooss, A., Dettmer, M.S., Altmann, K.-H., Gertsch, J., and Charles, R.-P. (2018). The LAT1 inhibitor JPH203 reduces growth of thyroid carcinoma in a fully immunocompetent mouse model. J. Exp. Clin. Cancer Res. 37, 234.

Jin, L., Li, D., Alesi, G.N., Fan, J., Kang, H.-B., Lu, Z., Boggon, T.J., Jin, P., Yi, H., Wright, E.R., et al. (2015). Glutamate dehydrogenase 1 signals through antioxidant glutathione peroxidase 1 to regulate redox homeostasis and tumor growth. Cancer Cell 27, 257–270.

Keast, D., Arstein, D., Harper, W., Fry, R.W., and Morton, A.R. (1995). Depression of plasma glutamine concentration after exercise stress and its possible influence on the immune system. Med. J. Aust. 162, 15–18.

Korangath, P., Teo, W.W., Sadik, H., Han, L., Mori, N., Huijts, C.M., Wildes, F., Bharti, S., Zhang, Z., Santa-Maria, C.A., et al. (2015). Targeting glutamine metabolism in breast cancer with aminooxyacetate. Clin. Cancer Res. 21, 3263–3273.

Kuhn, K.S., Schuhmann, K., Stehle, P., Darmaun, D., and Fürst, P. (1999). Determination of glutamine in muscle protein facilitates accurate assessment of proteolysis and de novo synthesis–derived endogenous glutamine production. Am. J. Clin. Nutr. 70, 484–489.

Luo, Y., Yoneda, J., Ohmori, H., Sasaki, T., Shimbo, K., Eto, S., Kato, Y., Miyano, H., Kobayashi, T., Sasahira, T., et al. (2014). Cancer usurps skeletal muscle as an energy repository. Cancer Res. 74, 330–340.

Löfberg, E., Gutierrez, A., Wernerman, J., Anderstam, B., Mitch, W.E., Price, S.R., Bergström, J., and Alvestrand, A. (2002). Effects of high doses of glucocorticoids on free amino acids, ribosomes and protein turnover in human muscle. Eur. J. Clin. Invest. 32, 345–353.

Moore, S.C., Lee, I.M., Weiderpass, E., Campbell, P.T., Sampson, J.N., Kitahara, C.M., Keadle, S.K., Arem, H., Berrington de Gonzalez, A., Hartge, P., et al. (2016). Association of leisure-time physical activity with risk of 26 types of cancer in 1.44 million adults. JAMA Intern. Med. 176, 816.

Newsholme, E.A., and Calder, P.C. (1997). The proposed role of glutamine in some cells of the immune system and speculative consequences for the whole animal. Nutrition 13, 728–730.

Nurjhan, N., Bucci, A., Perriello, G., Stumvoll, M., Dailey, G., Bier, D.M., Toft, I., Jenssen, T.G., and Gerich, J.E. (1995). Glutamine: a major gluconeogenic precursor and vehicle for interorgan carbon transport in man. J. Clin. Invest. 95, 272–277.

Parry-Billings, M., Leighton, B., Dimitriadis, G.D., Curi, R., Bond, J., Bevan, S., Colquhoun, A., and Newsholme, E.A. (1991). The effect of tumour bearing on skeletal muscle glutamine metabolism. Int. J. Biochem. 23, 933–937.

Patterson, B.W., Horowitz, J.F., Wu, G., Watford, M., Coppack, S.W., and Klein, S. (2002). Regional muscle and adipose tissue amino acid metabolism in lean and obese women. Am. J. Physiol. Endocrinol. Metab. 282, E931–E936.

Pedersen, L., Idorn, M., Olofsson, G.H., Lauenborg, B., Nookaew, I., Hansen, R.H., Johannesen, H.H., Becker, J.C., Pedersen, K.S., Dethlefsen, C., et al. (2016). Voluntary running suppresses tumor growth through epinephrine-and IL-6-dependent NK cell mobilization and redistribution. Cell Metab. 23, 554–562.

Plumley, D.A., Souba, W.W., Hautamaki, R.D., Martin, T.D., Flynn, T.C., Rout, W.R., and Copeland, E.M. (1990). Accelerated lung amino acid release in hyperdynamicseptic surgical patients. Arch. Surg. 125, 57.

Porporato, P.E. (2016). Understanding cachexia as a cancer metabolism syndrome. Oncogenesis 5, e200–e210.

dos Santos, R.V.T., Caperuto, E.C., de Mello, M.T., Batista, M.L., and Rosa, L.F.B.P.C. (2009). Effect of exercise on glutamine synthesis and transport in skeletal muscle from rats. Clin. Exp. Pharmacol. Physiol. 36, 770–775.

Schrock, H., Cha, C.M., and Goldstein, L. (1980). Glutamine release from hindlimb and uptake by kidney in the acutely acidotic rat. Biochem. J. 188, 557–560.

Schulte, M.L., Fu, A., Zhao, P., Li, J., Geng, L., Smith, S.T., Kondo, J., Coffey, R.J., Johnson, M.O., Rathmell, J.C., et al. (2018). Pharmacological blockade of ASCT2-dependent glutamine transport leads to anti-tumor efficacy in preclinical models. Nat. Med. 24, 194–202.

Souba, W.W., Strebel, F.R., Bull, J.M., Copeland, E.M., Teagtmeyer, H., and Cleary, K. (1988). Interorgan glutamine metabolism in the tumor-bearing rat. J. Surg. Res. 44, 720–726.

Wu, G. (1998). Intestinal mucosal amino acid catabolism. J. Nutr. 128, 1249–1252.

Yang, Y., Yang, H.H., Hu, Y., Watson, P.H., Liu, H., Geiger, T.R., Anver, M.R., Haines, D.C., Martin, P., Green, J.E., et al. (2017). Immunocompetent mouse allograft models for development of therapies to target breast cancer metastasis. Oncotarget 8, 30621–30643.

Zhang, G., Liu, Z., Ding, H., Miao, H., Garcia, J.M., and Li, Y.P. (2017). Toll-like receptor 4 mediates Lewis lung carcinoma-induced muscle wasting via coordinate activation of protein degradation pathways. Sci. Rep. 7, 1–8.

Zhou, X., Wang, J.L., Lu, J., Song, Y., Kwak, K.S., Jiao, Q., Rosenfeld, R., Chen, Q., Boone, T., Simonet, W.S., et al. (2010). Reversal of cancer cachexia and muscle wasting by ActRIIB antagonism leads to prolonged survival. Cell 142, 531–543.

Supplemental Information

Exercise-Mediated Lowering of Glutamine

Availability Suppresses Tumor Growth

and Attenuates Muscle Wasting

Katrine S. Pedersen, Francesco Gatto, Bo Zerahn, Jens Nielsen, Bente K. Pedersen, Pernille Hojman, and Julie Gehl
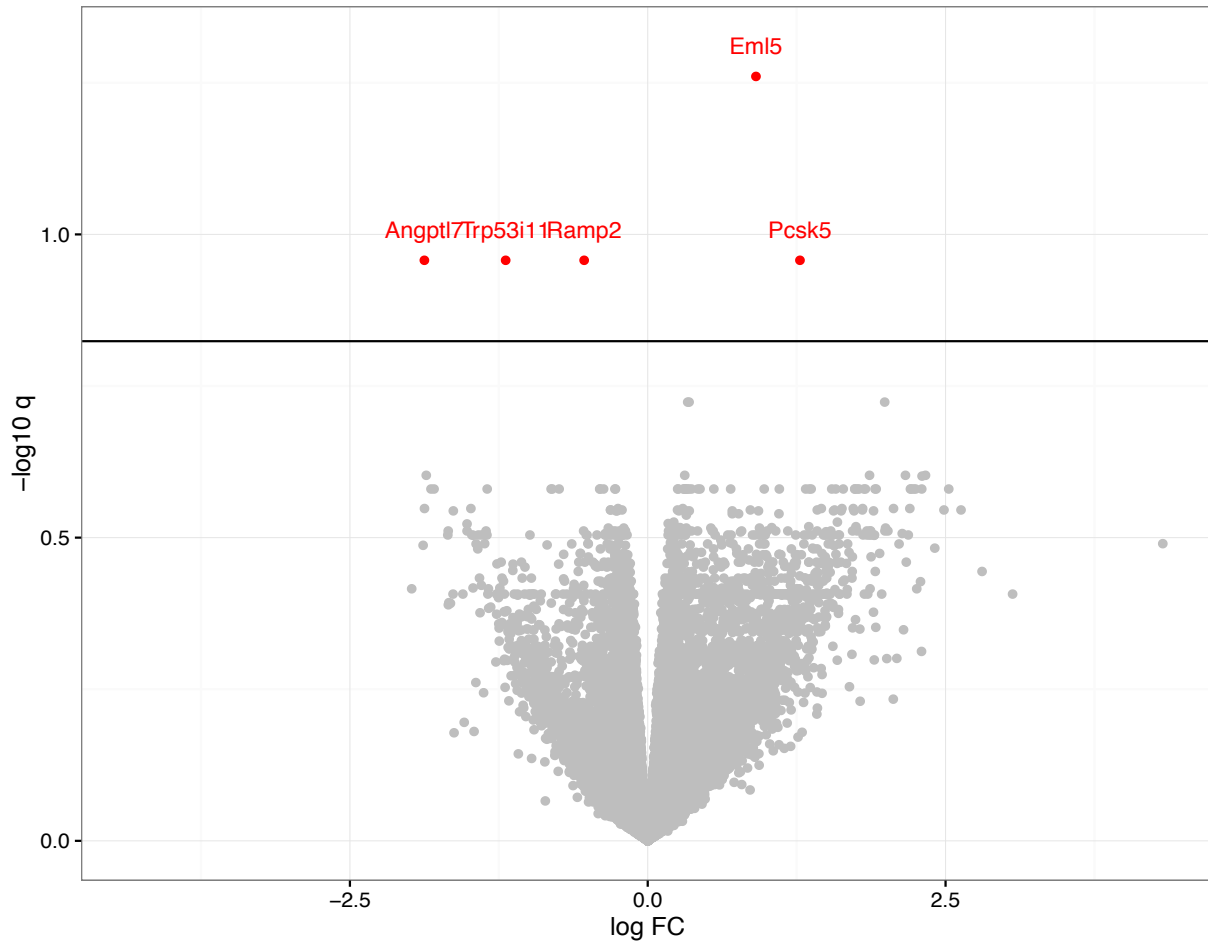
FIGURE S1. Volcano plot of RNAseq data from LLC tumors. Related to figure 4
Volcano plot of intratumoral gene expression obtained by RNA-sequencing of LLC tumors from sedentary (CON) and wheel running (EX) C57BL/6 mice (CON = 8, EX = 7). The y and x axes represent significance and log-fold-change, respectively. Red color designates genes that are significantly regulated in response to wheel running.

FIGURE S2. Volcano plot of RNAseq data from tibialis anterior muscles. Related to figure 6

Volcano plot of intramuscular gene expression obtained by RNA-sequencing of Tibialis Anterior muscle from sedentary (CON) and wheel running (EX) C57BL/6 mice carrying LLC tumors grown to the same size (CON = 10, EX = 14 (samples selected based on which mice ran the most)). The y and x axes represent significance and log-fold-change, respectively. Red color designates genes that are significantly regulated in response to wheel running.

TRANSPARENT METHODS

ANIMAL STUDIES

Mice

Mice were bred locally in the animal facilities using C57BL/6 breeding pairs purchased from Taconic Bioscience (Denmark) or Harlan (The Netherlands). For the study with MSO treatment, experimental mice were obtained directly from Taconic Bioscience, Denmark. All animal experiments were carried out in accordance with the ARRIVE guidelines, and protocols were approved by the Danish Animal Experiments Inspectorate. All animal experiments were carried out under controlled temperature and humidity conditions in a 12:12-h light-dark cycle. Adult female mice (16 weeks old for the wheel running experiment in mice with E0771 breast cancer tumors and aged 8-16 weeks for all other experiments) were housed in pairs in standard housing cages with free access to water and food.

Tumor models

LLC and E0771 tumor cell lines were tested negative for viruses and bacteria, including mycoplasma, by RAPIDMAP27-testing. For glutamine deprivation studies, LLC and E0771 cells were grown in RPMI 1640 culture medium with and without glutamine (ThermoFischer). Cell viability was measured by MTS assay with absorbance at 490 nm read in the Multiskan-Ascent ELISA reader (ThermoLabsystems). In preparation of tumor inoculations, LLC cells were grown in Dulbecco's Modified Eagle Medium (DMEM) (1X), Glutamax^{TM} (Gibco), and E0771 cells were grown in RPMI 1640 culture medium (ThermoFischer). All cells were grown in 10 cm dishes (ThermoScientific) at 37°C and 5% CO_2, and all media were supplemented with 10% fetal bovine serum (FBS) (Gibco) and 1% Penicillin/Streptomycin (P/S) (ThermoFischer). For tumor induction, LLC cells were inoculated subcutaneously at the flank ($2.5*10^5$ cells in 100 µl PBS/mouse). E0771 cells were inoculated in the mammary fat pad ($1*10^5$ cells in 100 µl PBS/mouse). For the wheel running and MSO studies, LLC and E0771 tumors were allowed to develop for 2-3 weeks before excision. Tumor size was determined by weight and by volume using the calculation $V=d_1*d_2*d_3*\pi/6$, where d is the diameter of the tumor. For the swimming experiment, E0771 tumors grew for 16 days before the swimming intervention.

MSO treatment

For the MSO experiments, mice received intraperitoneal injections of L-Methionine Sulfoximine, (M5379, Sigma) or saline from 2 weeks before tumor cell inoculation and until termination. MSO was dissolved in 0.9% saline and administered intraperitoneally 3x/week (Mondays, Wednesdays and Fridays) at a dose of 20 mg/kg mouse.

Exercise interventions

For the voluntary wheel running intervention, running wheels (Starr Life Sciences) of 12 cm in diameter were installed in the home cages from 4 weeks before tumor cell inoculation and throughout the experiment. Both mice from one cage could run in a wheel simultaneously. Running distance was measured daily by LCD Activity Wheel Counters (Starr Life Sciences), and cages that did not exceed 0.5 km/day/mouse were excluded from the exercise groups.

For the swimming interventions, mice were placed in a 35°C water basin to swim for 45 min as a model of acute exercise. For baseline blood samples, mice had blood drawn from the jaw and were given a resting period of 5 min before swimming. Subsequent blood samples were drawn either from the jaw (Fig. 3A) or from the neck after sacrifice (Fig. 3B).

DXA scanning

Fat mass (FM) and lean body mass (LBM) were determined using a LUNAR iDXA dual-energy X-ray absorptiometry (DXA) scanner (GE Healthcare Systems, LUNAR, Madison WI) with the "small animal" software application (acquisition software version 14.10.022 and analysis version 17). Mice were anaesthetized (Hypnorm/Dormicum, 0.1ml/10g) and placed side-by-side on the scan table. Each group of mice was scanned 5 consecutive times. Regions of interest (ROIs) for analysis of whole-body composition were manually adjusted once around each mouse and then copied to following scans. An overall threshold level for separation of bone from soft tissue was determined visually and kept for all scans in order to enable determination of relative changes in body composition. Median FM and LBM for each mouse were then calculated.

CELL LINES AND IN VITRO STUDIES

Differentiation and stimulation of C2C12 myotubes

Undifferentiated myoblasts were grown in Matrigel-coated dishes in growth medium (DMEM (1X) Glutamax (Gibco) supplemented with 20% FBS (Gibco), 1% Fungizone (Invitrogen) and 1% P/S (ThermoFischer)). At 90-100% confluence growth medium was substituted with differentiation medium (DMEM (1X) Glutamax (Gibco) supplemented with 2% HS (Gibco) and 1% P/S. Differentiation medium was replaced every day by removal of 90% of the old differentiation medium and addition of the same volume of fresh differentiation medium. For formation of fully differentiated myotubes for stimulation with myostatin and glutamine, differentiation proceeded for 7 days.

For incubation with myostatin, fully differentiated C2C12 myotubes were incubated for 2.5 h in normal differentiation medium with and without 400 ng/ml recombinant Myostatin (R&D Systems). For incubations in different glutamine concentrations, fully differentiated C2C12 myotubes were incubated for 2.5 hours in normal differentiation medium as described above (3.9 mM Glutamine) or in glutamine-free medium (DMEM (Gibco) supplemented with 2% HS and 1% P/S) with and without supplementation of 0.5mM L-Glutamine (Gibco). For incubation of differentiating myotubes in cancer cell conditioned medium, myotubes were differentiated under normal conditions for 96 hours as described above. Subsequently, differentiation was continued for 72 hours in medium containing 25% preconditioned medium from LLC cell cultures

Generation of LLC cell-conditioned medium

LLC cells were grown in DMEM) (1X), Glutamax^{TM} (Gibco), supplemented with 10% FBS and 1% P/S). Medium conditioned for 48h was collected and spun at 1000 G for 5 minutes (ROTOFIX 32A, Hettich Labinstrument ApS) to remove cell debris. Conditioned medium was mixed 1:4 in fresh C2C12 differentiation medium and added to myotubes as described above. The concentration of LLC cells when conditioned medium was collected was $651*10^3$ cells/ml as measured on the Countess^{TM} II FL Automated Cell Counter.

Fluorescence Microscopy

C2C12 myotubes were fixed and permeabilized using the Image-iT Fixation/Permeabilization Kit (Molecular Probes) and incubated with primary antibody for 1 hour at RT (1:50 Primary Anti-Sarcomeric Alpha Actinin antibody [EA-53] (ab9465) in Hanks Balanced Salt Solution (HBSS). Myotubes were washed 3x5 minutes in Dulbecco's Phosphate-Buffered Saline (DPBS) followed by incubation with secondary antibody (Alexa Flour Secondary antibodies (Molecular probes) under a lid for 30 minutes at room temperature. Myotubes were washed 3x5 minutes in DPBS before fluorescence microscopy in the EVOS FL (Thermo Fisher).

METHOD DETAILS

Serum glutamine measurements

Serum was generated by incubation of fresh blood samples at room temperature for 30 minutes, followed by centrifugation for 10 min at 3000 G at 4 °C. Glutamine was measured using the ENZYChrom^{TM} Glutamine Assay Kit (EGLN-100) (Bioassay Systems).

RNA isolation, cDNA synthesis and RT-qPCR

Upon excision, tumor and muscles were snap frozen in liquid nitrogen, and stored at -80°C. Before RNA extraction, frozen tumors were pulverized on dry ice using mortar and pestle. RNA was isolated from muscle and tumor tissue, or C2C12 myotubes by Ambion™ TRIzol™ Reagent (Invitrogen) according to manufacturer's instructions, dissolved in Ultrapure Nuclease free water (Life Technologies) and stored at -80°C until further use. RNA concentration and purity were measured on Nanodrop 1000 spectrophotometer (Thermo Scientific). Each sample was diluted to a final concentration of 25 ng/µl in a total volume of 10 µl Ultrapure Nuclease free water. Complementary DNA (cDNA) was synthesized using the High-Capacity cDNA Reverse Transcription Kit (Life Technologies) in the S1000TM Thermal Cycler (BioRad), diluted with Ultrapure Nuclease free water to a final volume of 200 µl and stored at -20°C. For RT-qPCR, samples were loaded in triplicates onto MicroAmp® Optical 384-Well Reaction Plates (Life Technologies), spun at 1000 G for 2 minutes in the (SIGMA 4-16KS bench centrifuge) and cDNA templates were amplified in the WiiA7 real-time PCR machine (Applied Biosystems) with either SYBR Green (PowerUp SYBR® Green PCR Master Mix, Applied Biosystems) or TaqMan (TaqMan®Universal PCR Master Mix, Applied Biosystems) master mix. Data was quantified using the delta/delta CT method, and expression levels of target genes were normalized to the reference genes glyceraldehyde-3-phosphate dehydrogenase (GAPDH) for muscle tissue or peptidylprolyl isomerase A (PPIA) for tumor tissue.

Murine primer sequences applied

Primer	Forward	Reverse	Probe
AR2A	TTTGTCTCCGAGGAAGACCC	TCTGCCAAGTATAGCACCTGA	
AR2B	GTGGACATCCATGAGGACCC	CACAGCCACAAAGTCGTTCA	
Atrogin1	CACATTCTCTCCTGGAAGGGC	TTGATAAAGTCTTGAGGGGAAAGTG	
GAPDH	AACTTTGGCATTGTGGAAGG	GGATGCAGGGATGATGTTCT	
GS	CCCCAAGGCCCGTATTACT	TAGTGAGCCTCCACGATGTC	
Myostatin	GGCCATGATCTTGCTGTAACC	GGTGTGTCTGTCACCTTGACTTCT	
Murf1	AACTGCTGGTGGAAAACATC	CCAGCATGGAGATGCAGTTA	6-FAM-CCAGGAGAAGATG-GGCTGAATCCCTTT-TAMRA
PPIA	GGGTTCCTCCTTTCACAGAA	GATGCCAGGACCTGTATGCT	5'-FAM-TGAGGTGCCTA-CTTGCTCCT-3-TAMRA3
SLC38A3	GCAGAAGGAGCCCACAATAC	TCAGGTATCTGTGCTCTGGA	
SLC1A5	CGCTATCGTCTTTGGTGTGG	CGGGTGCGTACCACATAATC	
SLC7A5	ATCTGGACGTGGGGAACATT	CAGGTTCCTGTAGGGGTTGA	
SMAD2	AGGAGCAGCTCGCCAAG	CGGTAAATCTACCCTCCGGG	
SMAD3	AGAAGCTCAAGAAGACGGGG	CAGTGACCTGGGGATGGTAAT	
SMAD7	AACCCCCATCACCTTAGTCG	CAGCCTGCAGTTGGTTTGAG	
PGC-1α-total	TGA TGT GAA TGA CTT GGA TAC AGA CA	GCT CAT TGT TGT ACT GGT TGG ATA TG	
PGC-1α-1	GGA CAT GTG CAG CCA AGA CTC T	CAC TTC AAT CCA CCC AGA AAG CT	
PGC-1α-2	CCA CCA GAA TGA GTG ACA TGG A	GTT CAG CAA GAT CTG GGC AAA	
PGC-1α-3	AAG TGA GTA ACC GGA GGC ATT C	TTC AGG AAG ATC TGG GCA AAG A	
PGC-1α-4	TCA CAC CAA ACC CAC AGA AA	CTG GAA GAT ATG GCA CAT	

RNA-sequencing analysis

RNA-seq was performed both on tumor and muscle tissues. In the latter case, all 10 mice from the tumor group were used, and the 14 mice having covered the most distance in the running wheels were selected from the Tumor + EX group. RNA was isolated from muscle and tumor tissue by Ambion™ TRIzol™ Reagent (Invitrogen). Sequencing libraries were prepared from 1µg total RNA using the TruSeq stranded mRNA library preparation kit (Cat# RS- 122-2101/2102, Illumina Inc.) including polyA selection. The library preparation was performed according to the manufacturers' protocol (#15031047). Sequencing was performed on HiSeq2500, paired-end 125bp read length with v4 sequencing chemistry. The following bioinformatics pipeline was adopted, as recommended by the sequencing facility. RNA-seq reads were trimmed for adapters using TrimGalore (*http://www.bioinformatics.babraham.ac.uk/projects/trim_galore*), aligned to GRcm38 ENSEMBLE *Mus musculus* genome using STAR (Dobin et al., 2013) and counted using featureCounts (Liao et al., 2014). Quality control (QC) was performed using MultiQC (Ewels et al., 2016) to check parameters such as frequency of duplicated reads, fraction of unaligned reads, saturation of known and number of unknown splice variants. Samples with <70% of reads aligned were considered of insufficient quality. Deposition of data: RNA-seq data related to tumor and muscle tissues were deposited in ArrayExpress: E-MTAB-5311 and ArrayExpress: E-MTAB-5974, respectively.

Differential gene expression and pathway analysis

For differential gene expression analysis, genes with less than 10 counts across the dataset were discarded. Read counts were normalized according to the library size into size-adjusted log-cpm (counts-per-million). Differential gene expression analysis was performed by fitting a weighted linear model to samples belonging to the two groups using voom and limma (Law et al., 2014). Genes differentially expressed at a false discovery rate (q) < 0.05 were considered statistically significant. In the case of tumor tissues, for which 15 of 16 samples passed QC, genes differentially expressed at a false discovery rate (q) < 0.15 were considered statistically significant. Pathway analysis was performed through multiple runs of gene-set analyses using piano R-package (Väremo et al., 2013). *Mus musculus* genes were converted 1-to-1 to human genes by homology. Ambiguous annotations were discarded (~66%). Hallmark pathways and Kyoto Encyclopedia of Genes and Genomes (KEGG) pathways were used as gene-set collections as retrieved in the Molecular Signatures Database (MSigDB) (Liberzon et al., 2015).

Western Blotting

Frozen muscle-samples were homogenized with a metal bullet in MG-buffer (10 % Glycerol, 20 mM Na-Pyrophosphate, 150 mM NaCl, 50 mM HEPES (pH 7,5) 1% NP-40, 20 mM β-glycerophosphate, 2 mM

Na$_3$VO$_4$, 10 mM NaF, 2mM PMSF (Isopropanol), 1 mM EDTA (pH 8), 1 mM EGTA (pH 8), 10 µg/ml Aprotinin, 10 µg/ml Leupeptin, 3 mM Benzamidine in dd-H$_2$0) in a Qiagen Tissue-lyser. The homogenate was rotated over end for 1h at 4 °C and centrifuged for 30 min at 17500 g at 4 °C. The supernatant was transferred to fresh Eppendorf-tubes, and protein concentration of the lysate was determined using PIERCE BCA Protein assay kit #23225.

Samples were diluted 3:1 in 4X Laemmli sample buffer containing 10% β-mercaptoethanol, and boiled for 5 min at 95 °C. Samples were separated by SDS PAGE on Criterion TGX Stain-free Precast Gels (Bio-Rad), transferred onto PVDF membranes (Trans-blot Turbo Transfer Pack, 0.2 um PVDF, Bio-Rad), blocked in 5% skimmilk in TBST 1h at RT and incubated with primary antibodies in 5% skimmilk in TBST ON at 4 °C. Membranes were washed 3x10 min in TBST before incubation with secondary antibody diluted in 5% skimmilk in TBST for 1h at RT, and imaged by the ChemiDoc Imaging System (Bio-Rad) after incubation with Lumina Forte Western HRP Substrate (Millipore) for 3-5 minutes. Bands were quantified using Image Lab software. The signal for the protein of interest in each lane was normalized to the total protein amount in the same lane visualized by fluorescent detection of proteins within the Criterion Stain Free gels. Primary antibodies: Goat-anti-MuRF1/TRIM63 (AF5366, R&D systems, 1:1000), rabbit-anti-Fbx32 (ab168372, Abcam, 1:1000), rabbit-anti-GLUL (D2O3F #80636, Cell Signaling, 1:1000), mouse-anti-SNAT3 (H-11), sc-398982, Santa Cruz, 1:1000). Secondary antibodies: Polyclonal Goat-anti-Rabbit immunoglobulins HRP (DAKO, 1:5000), Polyclonal Rabbit-anti-Mouse immunoglobulins HRP (DAKO, 1:5000), Polyclonal Rabbit-anti-Goat immunoglobulins HRP (DAKO, 1:500).

QUANTIFICATION AND STATISTICAL ANALYSIS

Statistical analyses (excluding RNAseq data) were performed using GraphPad Prism 7 Software. Differences between groups were analyzed for significant differences using paired and unpaired Student's t-tests and One-way and Two-way ANOVAs. Data in graphs represent mean +/- standard deviations, and p-values below 0.05 were considered significant. *$p<0.05$, **$p<0.01$, ***$p<0.001$.

DATA AND CODE AVAILABILITY

The accession number for the RNA-sequencing analysis of LLC tumor tissue reported in this paper is ArrayExpress: E-MTAB-5311. The accession number for the RNA-sequencing analysis of murine muscle tissue reported in this paper is ArrayExpress: E-MTAB-5974.

KEY RESOURCES TABLE

REAGENT or RESOURCE	SOURCE	IDENTIFIER
Antibodies		
Primary Anti-Sarcomeric Alpha Actinin antibody [EA-53]	Abcam	ab9465
Bacterial and Virus Strains		
None		
Biological Samples		
None		
Chemicals, Peptides, and Recombinant Proteins		
L-Methionine Sulfoximine	Sigma Aldrich	Cat#: M5379
Myostatin	R&D Systems	Cat#: 788-G8-010
Critical Commercial Assays		
ENZYChrom™ Glutamine Assay Kit	Bioassay Systems	EGLN-100
High-Capacity cDNA Reverse Transcription Kit	Life Technologies	Cat#: 4368814
PowerUp SYBR® Green PCR Master Mix	Applied Biosystem	Cat#: A25780
TaqMan®Universal PCR Master Mix	Applied Biosystems	Cat#: 4304437
TruSeq stranded mRNA library preparation kit	Illumina Inc.	RS- 122-2101/2102,
Deposited Data		
RNA-seq data related to tumor were deposited in ArrayExpress with project ID E-MTAB-5311		
RNA-seq data related to muscle tissues were deposited in ArrayExpress with project E-MTAB-5974		
Experimental Models: Cell Lines		
Lewis Lung carcinoma	ATCC	Cat#: ATCC® CRL-1642
E0771 breast cancer cell line	CH3 Biosystems	Cat#: 940001
Experimental Models: Organisms/Strains		
C57Black/C mice	Taconic	N/A
Oligonucleotides		
Please see Table S3 for PCR primers		

Recombinant DNA		
None		
Software and Algorithms		
Body composition with the "small animal" software application (acquisition software version 14.10.022 and analysis version 17)	GE Healthcare Systems, LUNAR, Madison WI	N/A
Other		
Running wheel (12 cm)	Starr Life Science	N/A
LCD Activity Wheel Counters	Starr Life Science	N/A